

Scattering of dislocated wavefronts by vertical vorticity and the Aharonov-Bohm effect I: Shallow water

CHRISTOPHE COSTE^a, MAKOTO UMEKI^b, and FERNANDO LUND^c

^a Laboratoire de Physique, ENS Lyon

46, Allée d'Italie 69364 Lyon Cedex 07, France

^bDepartment of Physics, University of Tokyo,

7-3-1 Hongo, Bunkyo-ku, Tokyo, 113 Japan

^cDepartamento de Física, Facultad de Ciencias Físicas y Matemáticas

Universidad de Chile, Casilla 487-3, Santiago, Chile

Abstract

When a surface wave interacts with a vertical vortex in shallow water the latter induces a dislocation in the incident wavefronts that is analogous to what happens in the Aharonov-Bohm effect for the scattering of electrons by a confined magnetic field. In addition to this global similarity between these two physical systems there is scattering. This paper reports a detailed calculation of this scattering, which is quantitatively different from the electronic case in that a surface wave penetrates the inside of a vortex while electrons do not penetrate a solenoid. This difference, together with an additional difference in the equations that govern both physical systems lead to a quite different scattering in the case of surface waves, whose main characteristic is a strong asymmetry in the scattering cross section. The assumptions and approximations under which these effects happen are carefully considered, and their applicability to the case of scattering of acoustic waves by vorticity is

noted.

03.40.Kf, 47.35.+i, 47.10.+g

I. INTRODUCTION

In a remarkable paper, Berry et. al. [1] clarified the way in which a curl-free magnetic vector potential modifies the wavefront structure of an electronic wavefunction that obeys the non relativistic Schrödinger equation. They concluded that for electrons travelling outside an infinitely long cylinder enclosing a magnetic field, the wavefronts outside the cylinder would be dislocated by an amount proportional to the amount of magnetic flux within the cylinder. Reasoning by analogy, they also concluded that such dislocated wavefronts should occur for surface water waves when they encounter a vortex. A simple experiment conclusively demonstrated this effect [1].

In the case of the electronic wavefunction interacting with a confined magnetic field (and its unconfined vector potential) Berry et. al. [1] also computed the complete solution to the Schrödinger equation that, in addition to the dislocated wave, includes a scattered wave. Trying to do this in the case of the water waves is however more difficult because the analogy between de Broglie waves and water waves breaks down when pushing it into a quantitative statement. There are two essential differences: The first is that for an electron the appropriate boundary condition is that the wave function vanishes at the surface of the cylinder; in the case of water waves, the waves of course penetrate inside the vortex and it becomes necessary to solve the appropriate equations not only outside the vortex but also inside, and match them with continuity conditions. The second is that the wave equations that govern both phenomena, although similar, differ in quantitative details. This paper addresses both these issues.

The scattering of surface waves by vertical vorticity in shallow water was discussed by Cerda and Lund [2] and by Umeki and Lund [3] who discovered that a vortex may support spiral wave solutions. Fabrikant and Raevsky [4] have studied the case of a fluid of arbitrary depth in a Born approximation. The interaction between surface waves and vertical vorticity is in many respects similar to that of acoustic waves and vorticity, a topic that has been much studied over the years and that recently has been the subject of particular interest

due to the possibility of using acoustic waves as a nonintrusive probe of vortical flows, both laminar and turbulent [5], much in the same way that X rays and neutrons are used to probe condensed matter structures, both ordered and disordered. Most treatments, however, rely on a Born approximation [6] whose validity breaks down when a surface wave interacts with a vertical vortex with nonvanishing circulation, leading to a long range velocity field that decays like $1/r$ where r is the distance to the vortex core. This is precisely the case that is studied in the present paper.

This paper is organized as follows: Section 2 derives the equations that describe the scattering of a surface wave by vertical vorticity in shallow water. We pay particular attention to the assumptions needed to derive those equations. Section 3 has a reminder on the Aharonov-Bohm effect as relevant for the present discussion. Section 4 presents the computation of the solution to the equations derived in Section 2. Section 5 presents several illustrative examples and Section 6 has concluding remarks. Technical details are contained in two Appendices. A subsequent paper [7] studies the first order corrections to the shallow water approximation.

II. SHALLOW WATER WAVES IN INTERACTION WITH A VERTICAL VORTEX

We consider the problem of the interaction of shallow water surface waves in an inviscid incompressible fluid of uniform depth h with a stationary vertical vortex. The coordinates are $(x, y) = \mathbf{x}$ in the horizontal direction and z in the vertical direction. The velocity and the surface displacement are denoted by $\mathbf{v}(\mathbf{x}, z, t) = (\mathbf{v}_\perp(\mathbf{x}, z, t), w(\mathbf{x}, z, t))$ and $\eta(\mathbf{x}, t)$, respectively.

The equation of motion is [8]

$$\partial_t \mathbf{v} + (\mathbf{v} \cdot \nabla) \mathbf{v} = -\rho^{-1} \nabla p - \mathbf{g}, \quad (2.1)$$

where ρ is the (uniform) density of the fluid, p is the pressure, \mathbf{g} is the gravitational acceleration, $\partial_t = \partial/\partial t$ and ∇ the three-dimensional gradient. The boundary conditions on w are

$w = 0$ at the fluid's bottom ($z = 0$), and

$$w = \partial_t \eta + \mathbf{v}_\perp \cdot \nabla_\perp \eta \quad (z = h + \eta(\mathbf{x}, t)), \quad (2.2)$$

where ∇_\perp is a horizontal gradient, at the surface. We consider a free surface and neglect surface tension, which is consistent with the shallow water approximation.

In shallow water the length scale for spatial variations is much bigger than the fluid depth h . Consequently, the continuity equation $\nabla \cdot \mathbf{v} = 0$ together with the boundary condition at the bottom imply

$$w(\mathbf{x}, zt)|_{z=h+\eta} = -\nabla_\perp \cdot \mathbf{v}_\perp|_{z=0} (h + \eta) \quad (2.3)$$

to leading order in h/L , where L is the length scale for space variations. Inserting (2.3) into the kinematic boundary condition (2.2) and using that, to leading order in the shallow water approximation

$$\mathbf{v}_\perp|_{z=0} = \mathbf{v}_\perp|_{z=h+\eta}$$

leads to

$$\partial_t \eta + h \nabla_\perp \cdot \mathbf{v}_\perp + \nabla_\perp \cdot (\eta \mathbf{v}_\perp) = 0, \quad (2.4)$$

assuming surface deformations small compared to depth ($\eta \ll h$).

Neglecting vertical accelerations with respect to \mathbf{g} , the z -component of (2.1) and continuity of the pressure at the free surface yield

$$p(\mathbf{x}, z, t) = \rho g(h + \eta(\mathbf{x}, t) - z) + p_a, \quad (2.5)$$

where p_a is the atmospheric pressure. Substitution into the \mathbf{x} -component of (2.1) gives, again in the shallow water approximation

$$\partial_t \mathbf{v}_\perp + (\mathbf{v}_\perp \cdot \nabla_\perp) \mathbf{v}_\perp = -g \nabla_\perp \eta. \quad (2.6)$$

We will consider surface waves with particle velocity $\mathbf{u}(\mathbf{x}, t)$ and surface deformation $\eta_1(\mathbf{x}, t)$ as small perturbations on a background flow consisting of a steady vertical vortex

$\mathbf{U}(\mathbf{x})$, with corresponding surface deformation $\eta_0(\mathbf{x})$; $u \ll U$, where U denotes a typical value of $\mathbf{U}(\mathbf{x})$, and $\eta_1 \ll \eta_0$. Substituting $\mathbf{v}_\perp = \mathbf{U}(\mathbf{x}) + \mathbf{u}(\mathbf{x}, t)$ and $\eta = \eta_0(\mathbf{x}) + \eta_1(\mathbf{x}, t)$ into (2.6) and (2.4) leads, to leading order in the small perturbations η_1 and \mathbf{u} , to

$$-g\nabla_\perp \eta_0 = (\mathbf{U} \cdot \nabla_\perp) \mathbf{U} = \frac{1}{2} \nabla_\perp U^2 - \mathbf{U} \times \text{rot} \mathbf{U}, \quad (2.7)$$

and

$$\mathbf{U} \cdot \nabla_\perp \eta_0 = 0. \quad (2.8)$$

These equations allow the computation of η_0 in terms of \mathbf{U} for the background flow. The first order equations are

$$\partial_t \mathbf{u} + (\mathbf{U} \cdot \nabla_\perp) \mathbf{u} = -(\mathbf{u} \cdot \nabla_\perp) \mathbf{U} - g\nabla_\perp \eta_1, \quad (2.9)$$

$$\partial_t \eta_1 + (\mathbf{U} \cdot \nabla_\perp) \eta_1 = -h\nabla_\perp \cdot \mathbf{u} \quad (2.10)$$

$$-[\eta_0 \nabla_\perp \cdot \mathbf{u} + (\mathbf{u} \cdot \nabla_\perp) \eta_0].$$

Taking the horizontal divergence of (2.9), we obtain

$$\partial_t \nabla_\perp \cdot \mathbf{u} + g\Delta_\perp \eta_1 = -\nabla_\perp \cdot [(\mathbf{U} \cdot \nabla_\perp) \mathbf{u} + (\mathbf{u} \cdot \nabla_\perp) \mathbf{U}], \quad (2.11)$$

where $\Delta_\perp = \nabla_\perp^2$, and rearranging the right hand side of (2.11) gives $(i, j = 1, 2)$

$$D_t \nabla_\perp \cdot \mathbf{u} + g\Delta_\perp \eta_1 = -2(\partial_i U_j)(\partial_j u_i), \quad (2.12)$$

where $D_t \equiv \partial_t + \mathbf{U} \cdot \nabla_\perp$. Taking the difference between D_t of Eqn. (2.11) and h times Eqn. (2.12) leads to

$$D_t^2 \eta_1 - c^2 \Delta_\perp \eta_1 = -D_t [\eta_0 \nabla_\perp \cdot \mathbf{u} + (\mathbf{u} \cdot \nabla_\perp) \eta_0] + 2h(\partial_i U_j)(\partial_j u_i), \quad (2.13)$$

where $c = \sqrt{gh}$ is the phase velocity of shallow water waves.

We consider the case $U \ll c$. In analogy with gas dynamics, we call $M = U/c$ the Mach number. We denote a typical length scale of the vortex by a , and the wavelength and

frequency of shallow water waves by λ and ν respectively. We will assume that wavelengths are small compared to vortex size [10]: $ka \equiv \beta \gg 1$, ($k = 2\pi/\lambda$).

Under these assumptions, the right hand side of (2.13) will be $O(M)$ or $O(\beta^{-1})$ compared with the left hand side. Neglecting these terms, the final equation to be solved is

$$D_t^2 \eta_1 - c^2 \Delta_\perp \eta_1 = 0. \quad (2.14)$$

Note that one might be tempted to neglect $(\mathbf{U} \cdot \nabla_\perp) \eta_1$ with respect to $\partial_t \eta_1$ on the grounds that $U \ll c$. However, it is possible to have $(\mathbf{U} \cdot \nabla_\perp) \eta_1 \sim \partial_t \eta_1$ without violating this small Mach number assumption by considering (as we do in Section 4 below) a background velocity $U \sim \omega a$ with length scale a and frequency scale ω , together with $\nu \gg \omega$ and $ka \gg 1$.

The equation (2.14) is readily obtained, under the same assumptions, in the diffusion of acoustic waves by a vortex [3]. The physics is the same since acoustic waves and shallow water waves are both *nondispersive*, and the results of Sections IV and V are valid for both types of waves. They depend only on two parameters, the dimensionless wave number β and the Mach number M , and when those parameters are the same the results that hold for the surface elevation η_1 may be transposed, quantitatively and with no change, for the scattered acoustic pressure.

III. ANALOGY WITH THE AHARONOV-BOHM EFFECT

The wave equation (2.14) possesses a close analogy with the quantum mechanical wave equation describing the Aharonov-Bohm effect, in which a magnetic vector potential influences the dynamics of a charged particle in a region where the magnetic field vanishes. This cannot happen in classical electrodynamics [9]. In its simplest form, this effect occurs when a beam of particles with charge q and mass m is incident normally on a long thin cylinder containing a magnetic field $\mathbf{B}(\mathbf{x})$ parallel to its axis. The Schrödinger equation in the presence of a magnetic vector potential \mathbf{A} is

$$\frac{1}{2m}(-i\hbar\nabla - q\mathbf{A}(\mathbf{x}))^2\psi(\mathbf{x}) = \frac{\hbar^2 k^2}{2m}\psi(\mathbf{x}), \quad (3.1)$$

where \hbar is Planck's constant. Outside the cylinder, $\mathbf{A}(\mathbf{x}) = (\Phi/2\pi r)\hat{\theta}$, with Φ the magnetic flux contained within the cylinder, and $\hat{\theta}$ an azimuthal unit vector. Of course, $\mathbf{B} = 0$ outside the cylinder.

Both Equations (2.14) and (3.1) allow for a solution of the form

$$\exp[-i(\mathbf{k} \cdot \mathbf{x} + \alpha\theta)],$$

where $\alpha = \nu\Gamma/(2\pi c^2) = k\Gamma/2\pi c$ in the fluid mechanics case and $\alpha = -q\Phi/2\pi\hbar$ in the quantum mechanics case. This is an exact statement in the latter case, while in the water wave case it is approximate, because (2.14) is valid only when $M \ll 1$ and $\beta \gg 1$. Except for integer values of α , this is a multivalued solution. Berry et. al. [1] showed how fixing this multivaluedness leads to a solution that is a superposition of dislocated wavefronts and scattered waves. This was achieved by solving the Schrödinger equation (3.1) with impenetrable boundary conditions: $\psi = 0$ at the surface of the cylinder. The appropriate boundary conditions in the fluids case are continuity of velocity and of surface elevation. We now turn our attention to solving Eqn. (2.14) under these conditions. One important physical difference between the classical and quantum mechanical cases is that in the latter the phase of the waves cannot be measured, while in the classical case it can. Table 1 compares these two cases.

IV. SCATTERING OF DISLOCATED WAVES BY A VORTEX

As an example, we consider a scattering problem by a circular uniform vortex with vorticity ω and radius a surrounded by an irrotational flow. Using polar coordinates (r, θ) , the background flow is given by [11]

$$\mathbf{U} = \begin{cases} \frac{1}{2}\omega r\hat{\theta} & \text{if } r \leq a \\ \frac{\Gamma}{2\pi r}\hat{\theta} & \text{if } r > a \end{cases} \quad (4.1)$$

where $\Gamma = \pi\omega a^2$ is the circulation. Eqn. (2.14) will be solved separately for $r < a$ and $r > a$, and the results matched with a continuity condition.

Inside the vortex we have, from (2.14),

$$[(\partial_t + (\omega/2)\partial_\theta)^2 - c^2(\partial_r^2 + (1/r)\partial_r + (1/r^2)\partial_\theta^2)]\eta_1 = 0. \quad (4.2)$$

We look for solutions that evolve harmonically (with a single global frequency ν) in time, and Fourier decompose them in the polar angle θ :

$$\eta_1 = \text{Re}[\sum_n \tilde{\eta}_{1n} e^{i(n\theta - \nu t)}], \quad (4.3)$$

where Re stands for the real part. Introducing this expression into (4.1) we obtain

$$\left(\frac{d^2}{dr^2} + \frac{1}{r} \frac{d}{dr} - \frac{n^2}{r^2} + k_n^2 \right) \tilde{\eta}_{1n} = 0, \quad k_n = \frac{|\nu - n\omega/2|}{c}. \quad (4.4)$$

Equation (4.4) has both Bessel and Neumann functions as solutions if $k_n \neq 0$. Regularity at the origin will exclude the latter. If $2\nu/\omega$ is an integer, $k_n (= k|1 - n/n_d|)$ vanishes for $n = n_d \equiv 2\nu/\omega$. In this case, (4.4) can be solved by assuming $\tilde{\eta}_{1n} \propto r^p$. Substituting this into (4.4), we have $p = \pm n$ and negative values of p are excluded, again because of regularity at the origin. Thus we have

$$\eta_1(r, \theta, t) = \text{Re} \left[\sum_{n \neq n_d} a_n \frac{J_{|n|}(k_n r)}{J_{|n|}(k_n a)} e^{i(n\theta - \nu t)} + C(n_d) a_{n_d} \left(\frac{r}{a} \right)^{n_d} e^{i(n_d \theta - \nu t)} \right], \quad (4.5)$$

where the a_n are as yet undetermined coefficients and $C(n_d) = 1$ when $2\nu/\omega$ is an integer and vanishes otherwise.

Outside the vortex, $r > a$, the assumption $U^2/c^2 \ll 1$ reduces (2.14) to

$$\left[\partial_t^2 + \frac{\Gamma}{\pi r^2} \partial_\theta \partial_t - c^2(\partial_r^2 + (1/r)\partial_r + (1/r^2)\partial_\theta^2) \right] \eta_1 = 0. \quad (4.6)$$

Inserting the form (4.3) of η_1 into this equation gives

$$\left(\frac{d^2}{dr^2} + \frac{1}{r} \frac{d}{dr} - \frac{n^2 + 2n\alpha}{r^2} + k^2 \right) \tilde{\eta}_{1n} = 0, \quad k = \frac{\nu}{c}. \quad (4.7)$$

with $\alpha = \nu\Gamma/2\pi c^2$. We wish this parameter to be of order 1. Following Berry et al. [1] we write the surface elevation outside the vortex in the form

$$\eta_1 = \text{Re}(\eta_{AB} + \eta_R), \quad (4.8)$$

where

$$\eta_{AB} = \sum_n b_n \frac{J_m(kr)}{J_m(\beta)} e^{i(n\theta - \nu t)}, \quad m \equiv \sqrt{n^2 + 2n\alpha}, \quad (4.9)$$

with $\beta \equiv ka$, and

$$\eta_R = \sum_n c_n \frac{H_m^1(kr)}{H_m^1(\beta)} e^{i(n\theta - \nu t)}. \quad (4.10)$$

The coefficients a_n , b_n and c_n are defined so that they denote the amplitude of the wave components at the vortex boundary $r = a$. In order to obtain these coefficients, the continuity of η and $\nabla_\perp \eta$ at $r = a$ is required. This gives two relations:

$$a_n = b_n + c_n, \quad (4.11)$$

$$a_n k_n \frac{J'_{|n|}(k_n a)}{J_{|n|}(k_n a)} = k \left(b_n \frac{J'_m(\beta)}{J_m(\beta)} + c_n \frac{H_m^{1'}(\beta)}{H_m^1(\beta)} \right). \quad (4.12)$$

If $n = n_d$, the corresponding relations are

$$a_n = b_n + c_n, \quad (4.13)$$

$$a_n \frac{n}{a} = k \left(b_n \frac{J'_m(\beta)}{J_m(\beta)} + c_n \frac{H_m^{1'}(\beta)}{H_m^1(\beta)} \right). \quad (4.14)$$

The third condition comes from the boundary condition of η at infinity. We require that the asymptotics of η_{AB} coincides with the dislocated wave incident from the right plus outgoing waves only. This leads to (see Appendix A)

$$\frac{b_n}{J_m(\beta)} = (-i)^m \quad (4.15)$$

Using the notation

$$\gamma_n \equiv \frac{k_n}{k} = \left| 1 - \frac{n\alpha}{\beta^2} \right|, \quad (4.16)$$

and the relationship $zZ'_\nu(z) = zZ_{\nu-1}(z) - \nu Z_\nu(z)$, where $Z_\nu(z)$ is any one of the Bessel functions, the following expressions for a_n and c_n are obtained, when $\gamma_n \neq 0$:

$$a_n = \frac{(-i)^m J_m(\beta)}{\Delta_n} \left[-\frac{H_{m-1}^1(\beta)}{H_m^1(\beta)} + \frac{J_{m-1}(\beta)}{J_m(\beta)} \right], \quad (4.17)$$

$$c_n = \frac{(-i)^m J_m(\beta)}{\Delta_n} \left[-\frac{\gamma_n J_{|n|-1}(\beta\gamma_n)}{J_{|n|}(\beta\gamma_n)} + \frac{J_{m-1}(\beta)}{J_m(\beta)} - \frac{1}{\beta}(m - |n|) \right], \quad (4.18)$$

where

$$\Delta_n = -\frac{H_{m-1}^1(\beta)}{H_m^1(\beta)} + \frac{\gamma_n J_{|n|-1}(\beta\gamma_n)}{J_{|n|}(\beta\gamma_n)} + \frac{1}{\beta}(m - |n|), \quad m = \sqrt{n^2 + 2n\alpha}. \quad (4.19)$$

If $\gamma_n = 0$, i.e., $n = n_d$, these formulae are replaced by

$$a_{n_d} = \frac{(-i)^{m_d} J_{m_d}(\beta)}{\Delta_{n_d}} \left[-\frac{H_{m_d-1}^1(\beta)}{H_{m_d}^1(\beta)} + \frac{J_{m_d-1}(\beta)}{J_{m_d}(\beta)} \right], \quad (4.20)$$

$$c_{n_d} = \frac{(-i)^{m_d} J_{m_d}(\beta)}{\Delta_{n_d}} \left[-(n_d + m_d)\beta^{-1} + \frac{J_{m_d-1}(\beta)}{J_{m_d}(\beta)} \right], \quad (4.21)$$

where

$$\Delta_{n_d} = -\frac{H_{m_d-1}^1(\beta)}{H_{m_d}^1(\beta)} + (m_d + n_d)\beta^{-1}, \quad m_d = \sqrt{n_d^2 + 2n_d\alpha}. \quad (4.22)$$

These expressions are the main algebraic result of this paper.

The limit $r \rightarrow \infty$ gives the surface elevation as

$$\begin{aligned} \eta_{AB} \rightarrow & e^{i(-kr \cos \theta + \alpha\theta - \nu t)} \\ & - \frac{ie^{i(kr - \nu t)} \sin \pi\alpha}{(2\pi ikr)^{1/2} \cos(\theta/2)} (-1)^{[\alpha]} e^{i([\alpha] + 1/2)\theta} \\ & + \frac{e^{i(kr - \nu t)}}{(2\pi ikr)^{1/2}} G(\theta, -\pi/2), \end{aligned} \quad (4.23)$$

where the function G is defined in Appendix A, and $[\alpha]$ denotes the integral part of α . The second term in the right hand side of the equation diverges for $\theta \rightarrow \pi$. This is because

this asymptotics is valid everywhere except in a narrow sector centered around the forward direction, $\theta = \pi$, of angular width $O(1/\sqrt{kr})$, where η_{AB} cannot be separated into incident and scattered waves [12], and it does not make sense to speak of a forward scattering amplitude. This peculiarity was already pointed out by Aharonov & Bohm [9] in the case of scattering by a *point* vortex.

Also

$$\eta_R \rightarrow \left(\frac{2}{\pi i k r} \right)^{1/2} e^{i(kr - \nu t)} \sum_n \frac{c_n}{H_m^1(\beta)} e^{i(n\theta - \pi m/2)}. \quad (4.24)$$

The sum of the last term of (4.23) and (4.24) is the correction to the Aharonov-Bohm scattering amplitude that comes from the matching of the surface elevation and of its gradient inside and outside the vortex core.

Berry et al. have calculated a correction for different boundary conditions. They consider the finite radius of the scattering solenoidal field, which is considered as impenetrable. In the quantum mechanical context, the scattering is due to the magnetic field inside the solenoid, and in an hydromechanical context it could be a solid body rotating in a perfect fluid. Their result reads [1]

$$\eta_R^{\text{Berry}} \rightarrow \left(\frac{2}{\pi i k r} \right)^{1/2} e^{i(kr - \nu t)} \sum_n \frac{J_{|n-\alpha|}(\beta)}{H_{|n-\alpha|}^1(\beta)} e^{i(n\theta - \pi |n-\alpha|)}. \quad (4.25)$$

Since the usual scattering cross section is not defined in the forward direction, it is interesting instead to compare the difference in the far-field correction to the Aharonov-Bohm wave function (obtained in the limit of zero cylinder thickness) calculated by Berry et. al. on the basis of Schrödinger equation, and our own calculations obtained on the basis of the fluids equations. The general asymptotic form of the scattered wave η_S is

$$\eta_S \sim f(\theta) r^{-1/2} e^{i(kr - \nu t)}, \quad (4.26)$$

with a scattering amplitude $f(\theta)$ given by

$$f(\theta) = \frac{1}{\sqrt{2\pi i k}} \tilde{f}(\theta). \quad (4.27)$$

In the following section, we will compare the correction to the Aharonov-Bohm scattering amplitude for a vortex, that is

$$\tilde{f}(\theta) = G(\theta, -\pi/2) + 2 \sum_n \frac{c_n}{H_m^1(\beta)} e^{in\theta} (-i)^m, \quad (4.28)$$

with the correction for an impenetrable solenoidal field,

$$\tilde{f}_{\text{Berry}}(\theta) = 2 \sum_n \frac{J_{|n-\alpha|}(\beta)}{H_{|n-\alpha|}^1(\beta)} e^{i(n\theta - \pi|n-\alpha|)}. \quad (4.29)$$

V. NUMERICAL EXAMPLES

The solutions we have obtained are parametrized by two dimensionless numbers: $\alpha = \nu\Gamma/2\pi c^2$ and $\beta = ka$. That is, for a given incident wave, they depend on vortex radius and circulation as independent parameters. The Mach number is related to α and β through $\alpha = M\beta$. Scaling radial distance with the vortex radius, $r' \equiv r/a$, the analytical expression of the surface displacement is summarized as follows:

$$\begin{aligned} \eta_1 &= \text{Re } \eta_c, \quad 0 < r' \leq 1 \\ \eta_c &= \sum_{n \neq n_d} a_n \frac{J_{|n|}(\gamma_n \beta r')}{J_{|n|}(\gamma_n \beta)} e^{i(n\theta - \nu t)} \\ &\quad + C(n_d) a_{n_d} r'^{n_d} e^{i(n_d \theta - \nu t)}, \end{aligned} \quad (5.1)$$

$$\begin{aligned} \eta_1 &= \text{Re}(\eta_{AB} + \eta_R), \quad r' > 1 \\ \eta_{AB} &= \sum_n (-i)^m J_m(\beta r') e^{i(n\theta - \nu t)}, \end{aligned} \quad (5.2)$$

$$\eta_R = \sum_n c_n \frac{H_m^1(\beta r')}{H_m^1(\beta)} e^{i(n\theta - \nu t)}. \quad (5.3)$$

where $m = \sqrt{n^2 + 2n\alpha}$.

We have numerically computed the total surface displacement given by (5.2-5.3) for several values of the parameters α and β . In order to approximate the series in (5.2-5.3) by a finite sum, it is necessary to estimate their convergence. This is done in Appendix B,

where it is shown that η_c is an absolutely and uniformly convergent series, and that η_{AB} and η_R are both absolutely and simply convergent series. As an illustration, absolute values of the coefficients a_n and c_n are plotted in Fig. 1.

Since convergence of the series expansions for η_{AB} and η_R is not uniform, the number of terms to keep in the infinite series depends on the value of r' . In practice, we compute the patterns of the surface displacement in the region $|x'|, |y'| \leq 5[(x', y') = (r' \cos \theta, r' \sin \theta)]$ by the finite sum of (5.2) and (5.3) with $|n| \leq 50$ for $\beta = 10$ and $|n| \leq 30$ for $\beta = 5$, but we keep more terms, $|n| \leq 90$ in (5.2). Fig. 2 shows the resulting displacements for $\beta = 5$ and $\alpha = 0.5, 1, 1.5, 2$, and Fig. 3 for $\beta = 10$ and the same values of α . The dislocation of the incident wavefronts by an amount equal to α is clearly visible. The outward travelling scattered wave is also visible. Note the strong interference patterns between scattered and incident wave.

Another illustration is given in Fig. 4, where we subtract to the total field the dislocated wave. The scattered wave appears as an outgoing cylindrical wave, with a clearly visible dislocation in the forward direction. This is the part of the wave that *does not* decrease as $1/\sqrt{kr}$, and that ensures single-valuedness of the total field. Note that the representation is for an half-integer value of α , and the scattering amplitude is exactly zero in the direction $\theta = \pi$ [1]; the comparison between the two figures clearly shows the exact compensation of the dislocation in this direction, because of destructive interference, to yield a single valued total wave field.

Finally, Fig. 5 shows the absolute value of the correction to the Aharonov-Bohm scattering amplitude, compared to the correction calculated by Berry et al. For $\alpha \geq 0.5$, the parameter m is imaginary for small negative n . This induces very different partial amplitudes for $\exp(-in\theta)$ and $\exp(in\theta)$ when n is small. Our calculations thus predict a forward scattering with a strong asymmetry, which increases with α as shown in Figs. 5 (c) and 5 (d). This asymmetry effect is observed both in experiments on water wave scattering by a vortex [13] and in direct numerical simulations of sound scattering by a vortex [14]. As can be seen from the dashed curves in Fig. 5, this asymmetry is absent in the calculation of

Berry et al. For $\alpha \leq 0.5$, the parameter m is real for all n and the scattering in the forward direction is much less asymmetric (Figs. 5 (a) and 5 (b)).

All calculations were performed using Mathematica [15].

VI. CONCLUDING REMARKS

We have computed the surface displacement due to a surface wave interacting with a vertical vortex in shallow water when the vortex core performs solid body rotation, the wavelength is small compared to the vortex core radius and the particle velocities associated with the wave are small compared with the particle velocities associated with the vortex. When the parameter $\alpha = \nu\Gamma/2\pi c^2$ is of order one or bigger, the wavefronts become dislocated. The scattered waves interact strongly with the dislocated wavefronts and produce interference patterns. The differential scattering cross section is strongly peaked along a direction at an angle with respect to the incident direction. This is in contrast with previous calculations of Berry et al. [1] in the case of quantum mechanical scattering by an impenetrable cylinder of finite radius. In the sequel to this paper [7], we will show that these properties roughly persist when the depth of the water increases. This is important because deep water waves are much more amenable to actual experiments.

ACKNOWLEDGMENTS

The work of F.L. is supported by Fondecyt Grant 1960892 and a Cátedra Presidencial en Ciencias. We gratefully acknowledge a grant from ECOS-CONICYT.

APPENDIX A: ASYMPTOTICS

In this Appendix, we study the asymptotic behavior of the function (4.9). To this end, we use the computations in the Appendix of Berry et. al.'s paper [1]. In order to avoid confusion, we use the following notations: Our definition of m is called $m_{\text{new}} \equiv \sqrt{n^2 + 2n\alpha}$,

whereas the function used in [1] is called $m_{\text{old}} \equiv |n + \alpha|$. Similarly, we note \tilde{b}_n the constants in the series representation of η_{AB} in our work, whereas the constants for η_{AB}^{Berry} are noted b_n .

Solutions to our Eqn. (4.7) are Bessel functions of order m_{new} . Moreover, the dislocated wave

$$\exp[-i(\vec{k} \cdot \vec{x} + \alpha\theta + \nu t)] \quad (\text{A1})$$

is a solution of Eqn. (2.14) asymptotically, that is for $kr \gg \alpha$. Consequently, it is appropriate to take as a boundary condition at large distances from the vortex that the solution should approach this dislocated wave.

Let us consider

$$\eta_{AB} = \sum_n \tilde{b}_n \frac{J_{m_{\text{new}}}(kr)}{J_{m_{\text{new}}}(\beta)} e^{i(n\theta - \nu t)}$$

Coefficients \tilde{b}_n should be determined from the boundary condition that η_{AB} should tend asymptotically to (A1) plus purely outgoing cylindrical waves. The representation

$$J_m(z) = \frac{1}{2\pi} \int_{-\pi+i\infty}^{\pi+i\infty} e^{i(mt - z \sin t)} dt \quad (\text{A2})$$

is still valid for $m = m_{\text{new}}$, even for those m 's that are purely imaginary (Ref. [16] p. 954, formula 8.412.6). This happens when α is bigger than 0.5, and for those n 's satisfying

$$-2\alpha < n < 0.$$

Next, we note that as n grows, with $\alpha \sim O(1)$, the difference between m_{old} and m_{new} decreases rapidly. Consequently, there will be an N , such that, if $n > N$, the difference between the two m 's will be smaller than any preassigned value. Let us write

$$\begin{aligned} \eta_{AB} = \eta_{AB}^{\text{point}} + \sum_{|n| < N} \left(\tilde{b}_n \frac{J_{m_{\text{new}}}(kr)}{J_{m_{\text{new}}}(\beta)} - b_n \frac{J_{m_{\text{old}}}(kr)}{J_{m_{\text{old}}}(\beta)} \right) e^{in\theta} + \\ + \underbrace{\sum_{|n| > N} \left(\tilde{b}_n \frac{J_{m_{\text{new}}}(kr)}{J_{m_{\text{new}}}(\beta)} - b_n \frac{J_{m_{\text{old}}}(kr)}{J_{m_{\text{old}}}(\beta)} \right) e^{in\theta}}_{\equiv R_N}. \end{aligned} \quad (\text{A3})$$

The wave η_{AB}^{point} is the original result of Aharonov & Bohm [9], and represents the scattering by a *point* vortex, hence the notation. The decomposition (A3) is interesting only if the last sum, R_N , is small when N is sufficiently large. We will see that it is indeed the case, and we temporarily drop it from the calculations.

We know that if

$$\frac{b_n}{J_{m_{\text{old}}}(\beta)} = (-i)^{m_{\text{old}}}$$

then η_{AB}^{point} gives a dislocated wavefront plus an outgoing cylindrical wave. Next, if

$$\frac{\tilde{b}_n}{J_{m_{\text{new}}}(\beta)} = (-i)^{m_{\text{new}}}$$

we may write,

$$\eta_{AB} = \eta_{AB}^{\text{point}} + \int_{-\pi+i\infty}^{\pi+i\infty} dt e^{-ikr \sin t} G(\theta, t)$$

where

$$G(\theta, t) \equiv \sum_{|n| < N} e^{in\theta} \left(e^{im_{\text{new}}(t-\pi/2)} - e^{im_{\text{old}}(t-\pi/2)} \right) \quad (\text{A4})$$

is an analytic function of t , because it is a finite sum of analytic functions (exponentials). Also, it is dominated by the contribution from low n 's. For $kr \rightarrow \infty$, η_{AB} can still be evaluated using steepest descent. Since G does not have any poles, the pole contribution to η_{AB} is the same as that of Berry et. al., namely Eqn. (A4) of [1]. This is good, since it is just the dislocated incident wave. Also, $G(t = \pi/2) = 0$ for all θ , including the forward and backwards directions. This means that there are no further contributions from the $t = \pi/2$ saddle point. This is also good, since the outgoing character of the scattered wave is preserved. On the other hand,

$$G(\theta, -\pi/2) = \sum_{|n| < N} e^{in\theta} \left(e^{-im_{\text{new}}\pi} - e^{-im_{\text{old}}\pi} \right).$$

This is different from zero for all θ , including the forward and backwards directions and we have, outside a small angular sector around the forward direction, the following asymptotic behaviour at large distances:

$$\eta_{AB}(r \rightarrow \infty) = \eta_{AB}^{\text{point}}(r \rightarrow \infty) + \frac{e^{ikr}}{\sqrt{2\pi ikr}} G(\theta, -\pi/2) \quad (\text{A5})$$

This result differs from that obtained by Berry et. al. [1] on the basis of Schrödinger's equation.

Let us turn back to the behavior of R_N at large N . We consider the behavior of

$$|R_N| < \sum_{|n|>N} |(-i)^{m_{\text{new}}-m_{\text{old}}} J_{m_{\text{new}}}(z) - J_{m_{\text{old}}}(z)| \quad (\text{A6})$$

where $z = kr$ is a fixed number. Using the asymptotic expressions of Bessel functions for large values of the index (Ref. [16], formula 8.452.1), we have

$$J_{|n+\alpha|}(z) \sim \frac{e^{|n+\alpha|(\tanh \delta_1 - \delta_1)}}{\sqrt{2\pi|n+\alpha|\tanh \delta_1}}, \quad |n+\alpha| \equiv z \cosh \delta_1, \quad (\text{A7})$$

$$J_{\sqrt{n^2+2n\alpha}}(z) \sim \frac{e^{\sqrt{n^2+2n\alpha}(\tanh \delta_2 - \delta_2)}}{\sqrt{2\pi\sqrt{n^2+2n\alpha}\tanh \delta_2}}, \quad \sqrt{n^2+2n\alpha} \equiv z \cosh \delta_2, \quad (\text{A8})$$

where \sim means that we consider only the dominant behavior at large n . An important point is that these expressions suppose that $n > z$. The following study concerns simple convergence of the series R_N , for a fixed value of z , not uniform convergence valid for all z .

We define

$$\epsilon = \frac{\alpha^2}{2z|n+\alpha|} = O(1/n),$$

so that large n behavior means small ϵ . It is easy to show that $\delta_2 \sim \delta_1 - \epsilon/\sinh \delta_1$, and that $\sqrt{n^2+2n\alpha} \sim |n+\alpha| - \epsilon z$. We then deduce that

$$(-i)^{m_{\text{new}}-m_{\text{old}}} \sim 1 + i\frac{\pi}{2}\epsilon z,$$

$$\sqrt{n^2+2n\alpha}(\tanh \delta_2 - \delta_2) \sim |n+\alpha|(\tanh \delta_1 - \delta_1) + \epsilon z \delta_1,$$

and that

$$\sqrt{n^2+2n\alpha} \tanh \delta_2 \sim |n+\alpha| \tanh \delta_1 - \epsilon z \cosh \delta_1 / \sinh \delta_1,$$

$$\delta_1 = \text{Argcosh} \frac{|n + \alpha|}{z} = O(\log n),$$

so that

$$\epsilon z \delta_1 = O(\log n/n) \ll 1$$

for large n . We have thus

$$(-i)^{m_{\text{new}} - m_{\text{old}}} J_{\sqrt{n^2 + 2n\alpha}}(z) - J_{|n+\alpha|}(z) \sim \epsilon z (\delta_1 + i\pi/2) J_{|n+\alpha|}(z) = O\left(\frac{\log n}{n} \frac{n^{-n}}{\sqrt{n}}\right)$$

Using only the very rough inequality $\log n/n\sqrt{n} < 1$, we can now conclude on the asymptotic behavior of R_N at large N . Beginning with (A6), we obtain

$$|R_N| < \sum_N^{\infty} N^{-n} < N^{-N} \quad (\text{A9})$$

up to prefactors that we have dropped. The important point is that, indeed, R_N is a very small correction at large N , which validates the preceeding analysis. As a last remark, we insist on the fact that all calculations are done for a *fixed value* of z , and that N , at a prescribed accuracy, may depend on z .

APPENDIX B: CONVERGENCE

In this appendix, we discuss the convergence of the numerical series (5.2-5.3).

The simplest case is that of η_{AB} . In this case, the variable r' may extend toward infinity, and we fix its value in the calculations. Therefore we can conclude only on simple convergence of the series, not uniform convergence. For large n , $m \sim n$. Using the formula (A7), and for a *fixed* value of $z' \equiv \beta r'$, the angle $\delta = O(\log n)$ and we get

$$J_m(z') \sim \frac{1}{\sqrt{n}} \left(\frac{e}{n}\right)^n,$$

so that most clearly the series (5.2) is absolutely simply convergent.

In the coefficients a_n and c_n , some functions depends on $\gamma_n \beta$, and from (4.16) we get $\gamma_n \beta \sim nM$ where $M \ll 1$ is the Mach number. Thus $\gamma_n \beta \ll n$, so that to get the asymptotic

behavior at large n of $J_n(\gamma_n\beta)$ we use the same formula (A7) as before, but the angle δ is now a constant of order one. We then deduce the asymptotic behavior of Δ_n from its expression (4.19)

$$\Delta_n = - \underbrace{\frac{H_{m-1}^1(\beta)}{H_m^1(\beta)}}_{=O(1)} + \underbrace{\frac{\gamma_n J_{|n|-1}(\beta\gamma_n)}{J_{|n|}(\beta\gamma_n)}}_{=O(n)} + \underbrace{\frac{1}{\beta}(m - |n|)}_{=O(1/n)} = O(n). \quad (\text{B1})$$

We have seen in the preceding paragraph that the convergence of $J_m(\beta)$ is extremely fast, which ensures convergence of a_n . For $0 \leq r' \leq 1$, the term $J_{|n|}(\gamma_n\beta r')/J_{|n|}(\gamma_n\beta)$ takes the maximum value at $r' = 1$ for sufficiently large values of n . Then the absolute convergence of the sum (5.2) is guaranteed by the absolute convergence of the coefficients a_n . Since the support of η_c is compact, this convergence is uniform.

Rather easily, we get that the asymptotic behavior of c_n is that of $J_m(\beta)$, which converges very rapidly. Let us introduce

$$\beta r' \equiv m / \cosh \delta_1, \quad \beta \equiv m / \cosh \delta_2.$$

We have that $\delta_1 < \delta_2$, both being asymptotically of order $\log n$. Using one more time the formula (A7), and its equivalent for Neumann functions (Ref. [16], formula 8.452.2), we get

$$\frac{H_m^1(\beta r')}{H_m^1(\beta)} \sim \frac{E_1 - iF_1}{E_2 - iF_2} \sim \exp[m(\delta_1 - \delta_2)]$$

where ($i = 1, 2$)

$$E_i \equiv \frac{\exp(m \tanh \delta_i - m \delta_i)}{\sqrt{2\pi m \tanh \delta_i}}$$

$$F_i \equiv \frac{\exp(m \delta_i - m \tanh \delta_i)}{\sqrt{\pi m \tanh \delta_i/2}}$$

which converges exponentially fast because $\delta_1 - \delta_2 < 0$. We deduce that η_R is an absolutely converging series. However, in this case, r' takes values in an infinite interval so that the convergence is only simple.

REFERENCES

- [1] M. V. Berry et. al., *Eur. J. Phys.* **1**, 154 (1980).
- [2] E. Cerda and F. Lund, *Phys. Rev. Lett.* **70**, 3896 (1993).
- [3] M. Umeki and F. Lund, *Flu. Dyn. Res.* **21**, 201 (1997).
- [4] A. L. Fabrikant and M. A. Raevsky, *J. Fluid Mech.* **262**, 141 (1994)
- [5] B. Derroncourt, J.-F. Pinton and S. Fauve, *Physica D*, to appear; M. Oljaca et. al. *Phys. Fluids A*, **10**, 886 (1998); A. Petrossian and J.-F. Pinton, *J. de Physique II (France)* **7**, 1 (1997); J. F. Pinton et. al., *J. de Physique II (France)* **3**, 3 (1993) C. Baudet, S. Ciliberto and J. F. Pinton, *Phys. Rev. Lett.* **67**, 193 (1991); H. Contreras and F. Lund, *Phys. Lett. A* **149**, 127 (1990); F. Lund and C. Rojas, *Physica D* **37**, 508 (1989); M. S. Howe, *J. Sound Vib.* **87**, 567 (1983) T. Kambe, *J. Japan Soc. Fluid Mech.* **1**, 149 (1982) (in japanese); P. R. Gromov, A. B. Ezerskii and A. L. Fabrikant, *Sov. Phys. Acoust.* **28**, 452 (1982); T. Kambe and U. Mya-Oo, *J. Phys. Soc. Japan* **50**, 3507 (1981).
- [6] An exception is the calculation of A. L. Fetter, *Phys. Rev.* **136**, A1488 (1964) for the scattering of sound by a vortex in the long wavelength approximation. In that work, long wavelength means both $\lambda \gg a$ and $\lambda \gg \Gamma/c$. The present paper considers the case (see text) $\lambda \ll a$, $\lambda \sim \Gamma/c$.
- [7] C. Coste and F. Lund, “Scattering of dislocated wavefronts by vertical vorticity and the Aharonov-Bohm effect II: Dispersive waves”, following paper.
- [8] L. D. Landau and E. M. Lifshitz, *Fluid Mechanics*, 2nd Ed., Pergamon (1987).
- [9] Y. Aharonov and D. Bohm, *Phys. Rev.* **115**, 485 (1959). For recent discussions, see R. M. Herman, *Found. of Phys.* **22**, 713 (1992) and L. O’Raifeartaigh, N. Strautman and A. Wipf, *Comments Nucl. Part. Phys.* **20**, 15 (1991).
- [10] See T. Colonius, S. K. Lele and P. Moin, *J. Fluid Mech.* **260**, 271 (1994) for a treatment

of this short wavelength limit using ray-tracing methods.

- [11] In this case, the restriction $u \ll U$ imposed in Section II will break down when r is very small or very large. At those points, however, the condition $u \ll c$, implicit in the derivation of Eqn. (2.14), assures that nonlinear terms can still be neglected.
- [12] As noted in [1], there is no singularity in the forward direction. For a more recent discussion within a Born approximation framework, see P. V. Sakov, *Acoust. Phys.* **39**, 280 (1993) and R. Berthet and F. Lund, *Phys. Fluids* **7**, 2522 (1995).
- [13] F. Vivanco and F. Melo, *Preprint* (1998).
- [14] R. Berthet, *unpublished* (1998).
- [15] S. Wolfram, *The Mathematica Book*, Third Edition, Cambridge University Press (1996).
- [16] I. S. Gradshteyn and I. M. Ryshik, *Table of Integrals, Series, and Products*, Academic, 1980.

FIGURES

FIG. 1. Plot of the absolute value of the coefficients a_n (a) and c_n (b) versus n in a log-linear scale for $(\alpha, \beta) = (0.5, 10)$, denoted by dots, $(\alpha, \beta) = (1.5, 10)$, denoted by empty circles, $(\alpha, \beta) = (0.5, 5)$, denoted by filled circles and $(\alpha, \beta) = (1.5, 5)$, denoted by empty squares. Note the asymmetry with respect to $n \rightarrow -n$

FIG. 2. Density plot of the surface elevation for the total wave patterns for $\beta = 5$, $\alpha = 0.5$: (a), $\alpha = 1$: (b), $\alpha = 1.5$: (c), $\alpha = 2$: (d). The greyscale is linear with surface amplitude (arbitrary units). The dark circle indicates the vortex location. Vortex rotation is counterclockwise. The box size is 10×10 in units of the vortex radius a . The incident wave comes from the right edge of the box. Note the dislocated wave, and the asymmetric scattering that occurs practically within a single quadrant.

FIG. 3. Same as figure 3, for $\beta = 10$, $\alpha = 0.5$: (a), $\alpha = 1$: (b), $\alpha = 1.5$: (c), $\alpha = 2$: (d).

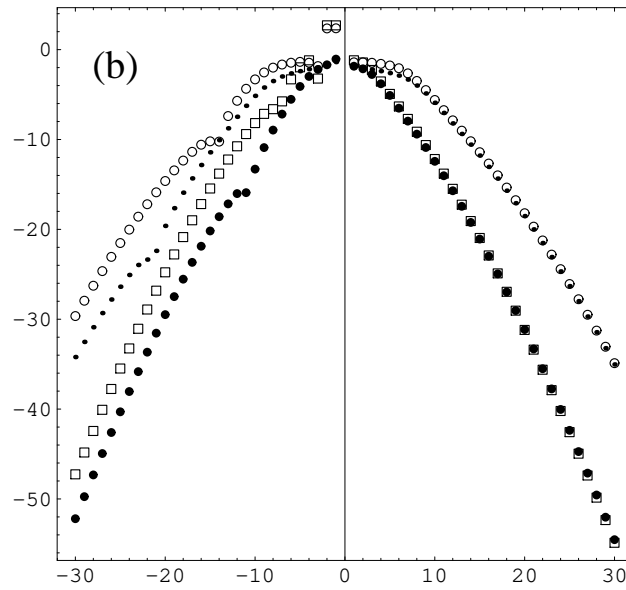
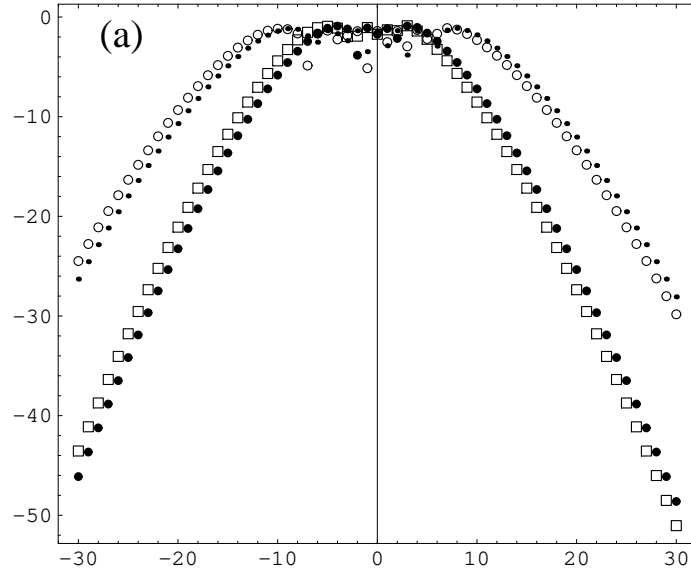
FIG. 4. Density plot of the surface elevation for a dislocated incident wave, with parameters $\alpha = 1.5$, $\beta = 5$ (resp. $\beta = 10$) : (a)[resp (c)], and for the difference between the total wave field with the same parameters, represented in Fig 2 (c) [resp. Fig 3 (c)] and the dislocated wave : (b)[resp. (d)]. Figures (b) and (d) correspond to the scattered wave generated by an incident dislocated wave. Such a scattered wave is itself dislocated in the forward direction, thus ensuring single valuedness.

FIG. 5. Polar plot of the absolute value of the correction to the Aharonov-Bohm (i.e. point) scattering amplitude, in the case of an impenetrable cylinder (dashed line) and in the case of a vortex (solid line), for $\beta = 10$ and $\alpha = 0.25$: (a), $\alpha = 0.5$: (b), $\alpha = 1$: (c), $\alpha = 1.5$: (d).

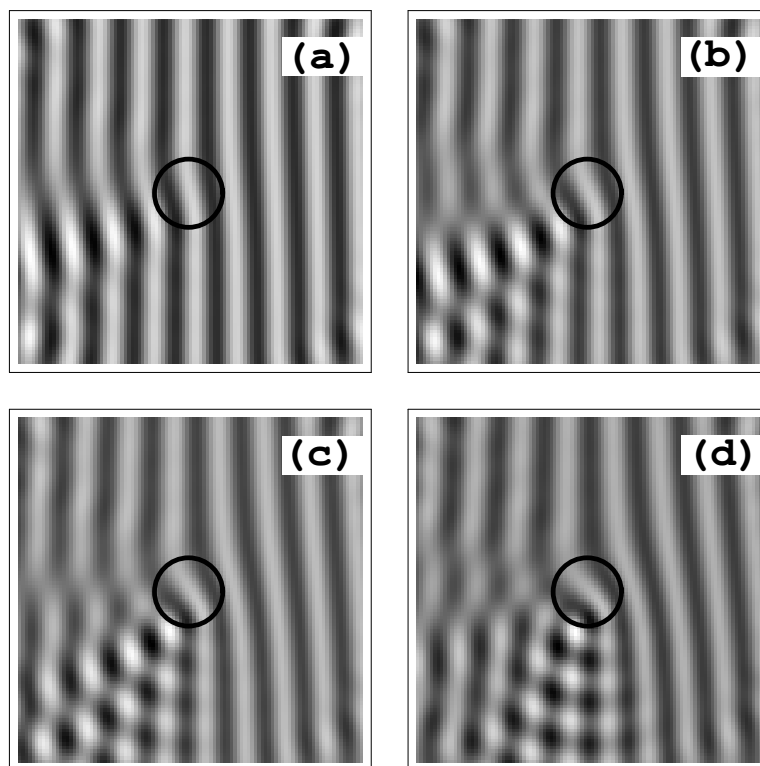
TABLES

TABLE I. Aharonov-Bohm effect in quantum and classical mechanics compared and contrasted.

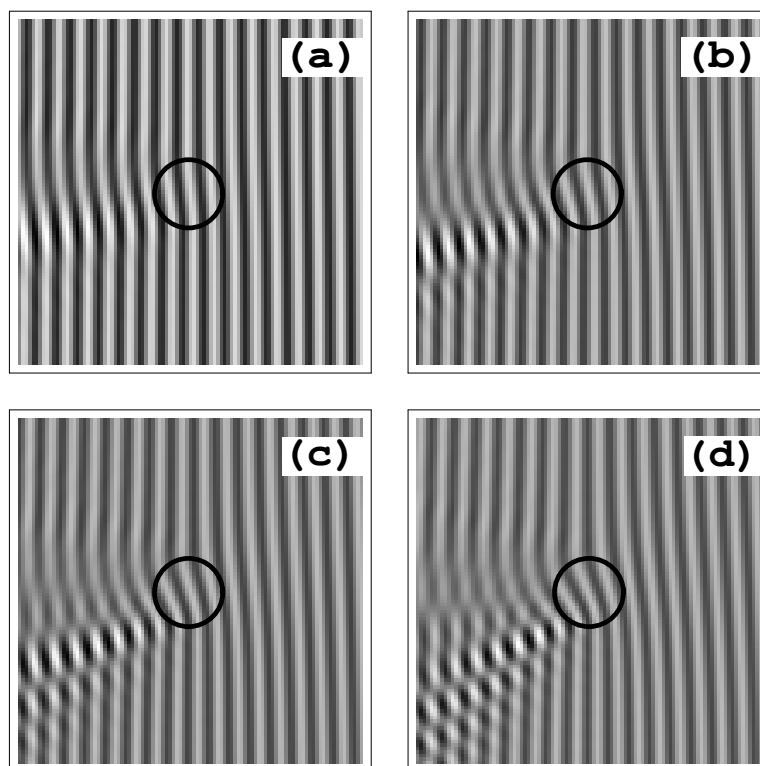
Quantum mechanics	Fluid mechanics
magnetic field $\mathbf{B} = \nabla \times \mathbf{A}$	vorticity $\boldsymbol{\omega} = \nabla \times \mathbf{U}$
vector potential \mathbf{A}	velocity \mathbf{U}
magnetic flux Φ	velocity circulation Γ
wave function ψ	surface displacement η
dislocation parameter $\alpha = -q\Phi/2\pi\hbar$	dislocation parameter $\alpha = k\Gamma/2\pi c$
dislocated wave is an exact solution	dislocated wave is approximate solution
phase is not measurable	phase is measurable



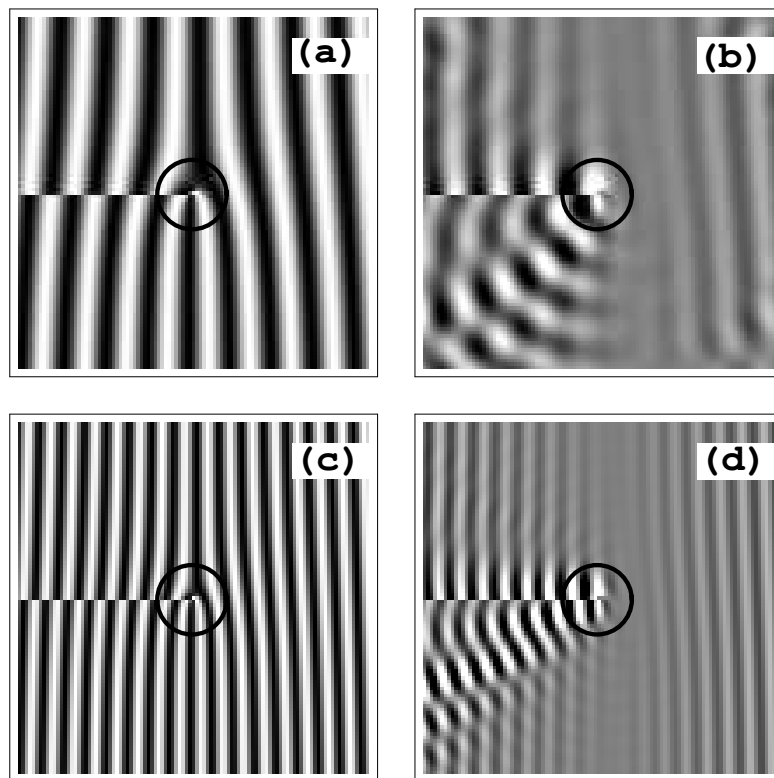
C. Coste *et al.*, Figure 1



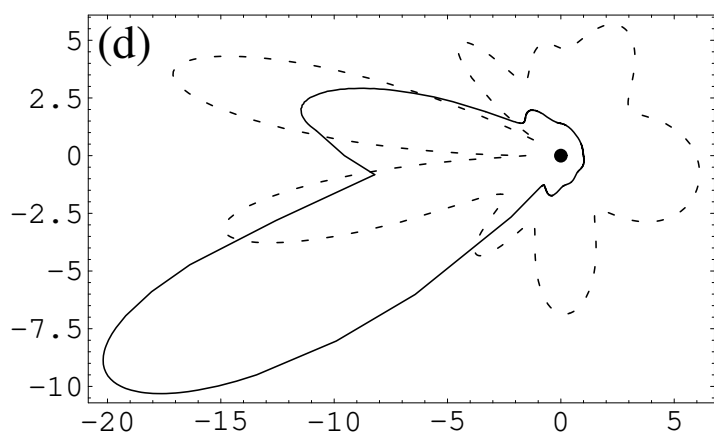
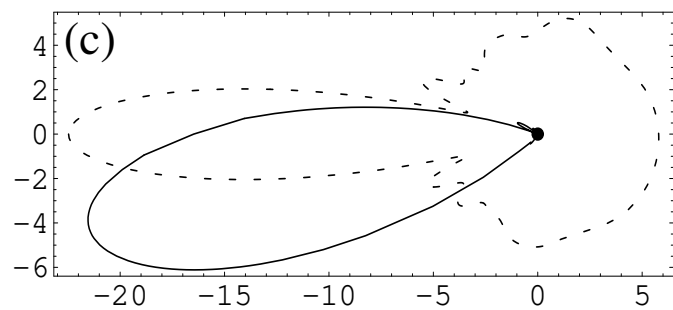
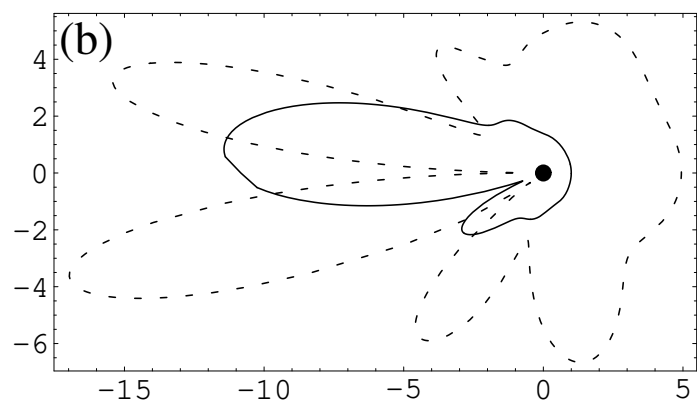
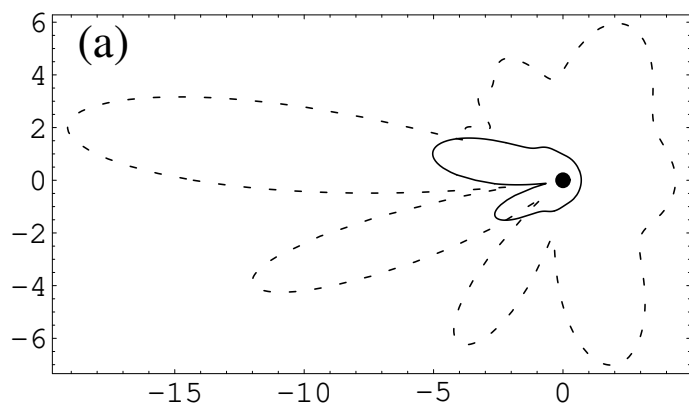
C. Coste *et al.*, Figure 2



C. Coste *et al.*, Figure 3



C. Coste *et al.*, Figure 4



C. Coste *et al.*, Figure 5